

# Integrative Analysis of DCE-MRI and Gene Expression Profiles in Construction of a Gene Classifier for Assessment of Hypoxia-Related Risk of Chemoradiotherapy Failure in Cervical Cancer

Christina S. Fjeldbo<sup>1</sup>, Cathinka H. Julin<sup>1</sup>, Malin Lando<sup>1</sup>, Malin F. Forsberg<sup>1</sup>, Eva-Katrine Aarnes<sup>1</sup>, Jan Alsner<sup>2</sup>, Gunnar B. Kristensen<sup>3,4,5</sup>, Eirik Malinen<sup>6,7</sup>, and Heidi Lyng<sup>1</sup>

## Abstract

**Purpose:** A 31-gene expression signature reflected in dynamic contrast enhanced (DCE)-MR images and correlated with hypoxia-related aggressiveness in cervical cancer was identified in previous work. We here aimed to construct a dichotomous classifier with key signature genes and a predefined classification threshold that separated cervical cancer patients into a more and less hypoxic group with different outcome to chemoradiotherapy.

**Experimental Design:** A training cohort of 42 patients and two independent cohorts of 108 and 131 patients were included. Gene expression data were generated from tumor biopsies by two Illumina array generations (WG-6, HT-12). Technical transfer of the classifier to a reverse transcription quantitative PCR (RT-qPCR) platform was performed for 74 patients. The amplitude  $A_{\text{Brix}}$  in the Brix pharmacokinetic model was extracted from DCE-MR images of 64 patients and used as an indicator of hypoxia.

**Results:** Classifier candidates were constructed by integrative analysis of  $A_{\text{Brix}}$  and gene expression profiles in the training cohort and evaluated by a leave-one-out cross-validation approach. On the basis of their ability to separate patients correctly according to hypoxia status, a 6-gene classifier was identified. The classifier separated the patients into two groups with different progression-free survival probability. The robustness of the classifier was demonstrated by successful validation of hypoxia association and prognostic value across cohorts, array generations, and assay platforms. The prognostic value was independent of existing clinical markers, regardless of clinical endpoints.

**Conclusions:** A robust DCE-MRI-associated gene classifier has been constructed that may be used to achieve an early indication of patients' risk of hypoxia-related chemoradiotherapy failure. *Clin Cancer Res*; 22(16); 4067–76. ©2016 AACR.

## Introduction

Improvements in the therapy of locally advanced cervical cancer are highly needed, as many patients experience local or systemic relapse and severe side effects after treatment (1, 2). Tumor hypoxia is an adverse factor associated with radiation resistance and metastasis (3–5). Thus, hypoxia is both a poten-

tial marker for predicting risk of recurrence and a target in new treatment strategies combined with radiotherapy. Adjuvant hypoxia-modifying treatment has been shown to improve the efficacy of radiotherapy in cervical cancer (6), and combination trials to find the optimal drug have been performed (7, 8) and are underway (ClinicalTrials.gov identifier NCT02394652). In many trials, difficulties in detecting drug effects and toxicity are major problems, as patients are randomized to the adjuvant treatment without knowledge of the hypoxia status of the tumor (9). Development of methods for classifying patients according to the hypoxia status is therefore an important requirement for reliable drug evaluation and to avoid added toxicity to patients with no expected benefit.

Gene expression signatures can provide an indirect measure of the hypoxia level in a tumor through the cellular transcriptional response to low oxygen concentrations and therefore be of value for classifier development. Several hypoxia signatures have been constructed in different tissues (10–18), but a common cancer signature seems difficult to derive (19). The only hypoxia signature presented for cervical cancer was discovered in our previous work by combining global gene expression profiles and dynamic contrast enhanced (DCE)-MRI of the same patients (20). The amplitude  $A_{\text{Brix}}$  in the Brix pharmacokinetic model (21) extracted from DCE-MR images was found by us and others to reflect hypoxia in cervical tumors

<sup>1</sup>Department of Radiation Biology, Norwegian Radium Hospital, Oslo University Hospital, Oslo, Norway. <sup>2</sup>Department of Experimental Clinical Oncology, Aarhus University Hospital, Aarhus, Denmark. <sup>3</sup>Department of Gynaecologic Oncology, Norwegian Radium Hospital, Oslo University Hospital, Oslo, Norway. <sup>4</sup>Institute for Cancer Genetics and Informatics, Norwegian Radium Hospital, Oslo University Hospital, Oslo, Norway. <sup>5</sup>Faculty of Medicine, University of Oslo, Oslo, Norway. <sup>6</sup>Department of Medical Physics, Norwegian Radium Hospital, Oslo University Hospital, Oslo, Norway. <sup>7</sup>Department of Physics, University of Oslo, Oslo, Norway.

**Note:** Supplementary data for this article are available at Clinical Cancer Research Online (<http://clincancerres.aacrjournals.org/>).

**Corresponding Author:** Heidi Lyng, Department of Radiation Biology, Norwegian Radium Hospital, Oslo University Hospital, Pb 4950 Nydalen, Oslo 0424, Norway. Phone: 472-293-1478; Fax: 472-278-1495; E-mail: heidi.lyng@rr-research.no

doi: 10.1158/1078-0432.CCR-15-2322

©2016 American Association for Cancer Research.

### Translational Relevance

Modification of tumor hypoxia is a promising strategy for therapy improvements of locally advanced cervical cancer. However, no successful combination of a modern hypoxia-targeted drug and radiation has so far been demonstrated. Methods for classifying patients according to hypoxia are lacking and are an important requirement for reliable drug evaluation and to avoid added toxicity to patients with no expected benefit. The presented DCE-MRI-associated prognostic 6-gene hypoxia classifier is a promising tool for identifying the patients with risk of hypoxia-related failure after conventional chemoradiotherapy. The classifier can be used in a prospective setting with data from an RT-qPCR assay. It is potentially applicable for routine use in clinical practice and may aid implementation of hypoxia-guided treatment strategies for the disease.

(20, 22). The signature contained 31 hypoxia-responsive genes, for which expression correlated with the patient-derived  $A_{\text{Brix}}$  data (20). This approach increased the likelihood of finding a signature that described a clinically relevant hypoxic phenotype. Both DCE-MRI and the 31-gene expression signature may have potential as a tool for assessing hypoxia in cervical cancer (20, 22). A current major limitation of MRI-based classifiers is, however, the lack of image standardization across MR machines (23, 24). Gene expression assays are easier to standardize, and multigene signatures have shown to be useful for guiding treatment decisions in many cancer types, like breast and prostate cancer (25, 26). Furthermore, gene signatures provide information that may increase the understanding of resistance mechanisms at play in individual tumors and thereby means for choosing the optimal targeted therapy in an individualized, combined radiotherapy regime (27).

Today, imaging and genomics appear as distinct facets in the treatment decision support system. Development of a direct link between the two disciplines would facilitate implementation of a multifactorial tool for a more accurate response prediction (24, 28). In this work, we aimed to prepare our signature for clinical use by constructing an image-associated, dichotomous hypoxia gene classifier with a predefined threshold for classification that could be utilized in a prospective setting. By integrative analysis of  $A_{\text{Brix}}$  and gene expression profiles, we identified genes in the signature that combined showed the optimal discrimination between more and less hypoxic tumors at the time of diagnosis. The power of this novel approach was demonstrated by the presentation of a hypoxia gene classifier that was reflected in DCE-MR images and showed prognostic impact across cohorts and test assays.

## Materials and Methods

### Patient cohorts, tumor specimens, and treatment

A total of 281 patients with locally advanced squamous cell carcinomas of the uterine cervix, prospectively recruited to our chemoradiotherapy protocol at the Norwegian Radium Hospital (Oslo, Norway) from 2001 to 2012, were included. Fifty-eight patients enrolled during the same period were not included because the tumor biopsies contained less than 50% malig-

nant cells in hematoxylin and eosin-stained sections from the central part of the specimen. The patients constituted three independent cohorts; training cohort ( $n = 42$ ), cohort 1 ( $n = 108$ ), and cohort 2 ( $n = 131$ ; Fig. 1; Supplementary Table S1). The patients were divided into the different cohorts based on the Illumina BeadArray version they were assayed by, that is, WG-6 v3 (training cohort, cohort 1) or HT-12 v4 (cohort 2). The patients assayed by the WG-6 arrays were further divided into the training cohort consisting of the patients with available  $A_{\text{Brix}}$  data and cohort 1 for the remaining patients. The patients were diagnosed in 2001 to 2004 for the training cohort, 2001 to 2009 (mainly 2004–2008) for cohort 1, and 2001 to 2012 (mainly 2005–2012) for cohort 2. The number of patients in cohort 1 and cohort 2 was sufficient for detecting an expected increase in the survival probability from 0.55 to 0.85 between more and less hypoxic tumors, respectively (20), with a power of 0.9 or larger ( $\alpha = 0.05$ ). Five additional patients with adenocarcinoma or adenosquamous carcinoma were included in the DCE-MRI analyses only. The study was approved by the Regional Committee for Medical and Health Research Ethics in southern Norway (S-01129). Written informed consent was achieved from all patients.

Tumor volume was determined from diagnostic MR images. Pathologic lymph nodes at diagnosis were also detected by MRI, or in a few cases by CT, according to the RECIST version 1.1 (29). One to four tumor biopsies (approximately  $5 \times 5 \times 5$  mm) were taken at diagnosis, immediately snap frozen, and stored at  $-80^{\circ}\text{C}$ . All patients received external radiation of 50 Gy to the primary tumor and elective areas and 45 Gy to the remaining pelvis in 25 fractions five times per week. Pathologic lymph nodes received additional 14 Gy. This was followed by brachytherapy of 25 Gy in 5 fractions. Concurrent cisplatin ( $40 \text{ mg/m}^2$ ) was given weekly in maximum 6 courses according to tolerance. Follow-up consisted of clinical examinations every third month for the first two years, twice a year for the next 3 years, and thereafter once a year. When symptoms of relapse were detected, MRI of pelvis and retroperitoneum as well as X-ray of thorax were performed. The study adheres to the REMARK criteria (30), and gene expression assays were performed blinded to the DCE-MRI results and clinical outcome.

### DCE-MRI

Diagnostic DCE-MR images of 64 patients (42 patients in the training cohort, 17 patients in cohort 2, and 5 patients with adenocarcinoma or adenosquamous carcinoma) were applied for construction and validation of the classifier (Fig. 1). Imaging was performed using a 1.5 T Signa Horizon LX tomography (GE Medical Systems) with a pelvic-phased array coil. The MR examination included standard T1 and T2-weighted imaging, followed by DCE-MRI with  $0.1 \text{ mmol/kg}$  body weight Gd-DTPA (Magnevist, Schering) administered as a fast bolus injection, as described previously (31). The uptake of contrast agent, that is, the relative signal intensity increase as a function of time after Gd-DTPA injection, was analyzed with the Brix pharmacokinetic model (21), and the amplitude  $A_{\text{Brix}}$  was derived for each tumor voxel (31). An  $A_{\text{Brix}}$  histogram was generated for each tumor, and the mean  $A_{\text{Brix}}$  value over the 20<sup>th</sup> to 30<sup>th</sup> percentile interval, which showed the strongest association to outcome in previous work (20), was calculated and used as an image parameter reflecting hypoxia.

### Cell culture

Hypoxia-induced genes were assessed in eight human cervical cancer cell lines from the ATCC: HeLa, SW756, C-33 A, C-4I, ME-180, HT-3, SiHa, and CaSki, and used for the first refinement of the signature. The cell lines were authenticated by STR/DNA profiling using PowerPlex 21 (Promega) by Eurofins Genomics. The cells were cultured at 37°C in a humidified 5% CO<sub>2</sub> incubator in DMEM with GlutaMAX (Gibco, Invitrogen) supplemented with 100 U/mL penicillin/streptomycin (Gibco) and 10% FCS. Cells were seeded in 10-cm plastic dishes (1–1.8 × 10<sup>6</sup> cells to obtain ~4 × 10<sup>6</sup> cells after 48 hours of incubation) 24 hours before exposure to hypoxic (0.2% O<sub>2</sub>, 5% CO<sub>2</sub>) or normoxic (95% air, 5% CO<sub>2</sub>) conditions for 24 hours at 37°C. The hypoxia treatment was performed in an Invivo2200 chamber (Ruskinn Technology).

### Gene expression by Illumina BeadArrays

Total RNA was isolated from frozen samples using TRIzol reagent (Invitrogen) (training cohort, cohort 1), miRNeasy Mini Kit (Qiagen; cohort 2), or RNeasy Mini Kit (Qiagen; cell lines). RNA from different biopsies of the same tumor was pooled. Gene expression profiling was performed using two different Illumina array generations; HumanWG-6 v3 (training cohort, cohort 1, cell lines) and HumanHT-12 v4 (cohort 2, adeno/adenosquamous carcinomas, cell lines; Illumina Inc.), both including approximately 48,000 transcripts. cRNA was synthesized, labeled, and hybridized to the arrays. Signal extraction and quantile normalization were performed using the software provided by the manufacturer (Illumina Inc.), and log<sub>2</sub>-transformed data were used in the analyses. The data were deposited in the gene expression omnibus database (GSE72723).

### Gene expression by reverse transcription quantitative PCR

The transferability of the classifier across assay platforms was tested in a reverse transcription quantitative PCR (RT-qPCR) assay on 74 patients from the training cohort and cohort 1, using the 7900HT Fast Real-Time PCR System (Applied Biosystems). Genomic DNA was removed from the RNA samples by using the DNA-free Kit (Ambion) according to the manufacturer's instructions. Reverse transcription was performed by the High-Capacity cDNA Reverse Transcription Kit (Life Technologies) with 2,000 ng DNase-treated RNA in a 20 µl reaction. 1 µl cDNA was amplified using TaqMan Fast Universal PCR Master Mix (2×) and Custom TaqMan Array 96-Well Fast Plates with dried-down TaqMan Assays (Life Technologies) for three reference genes: that is, *CHCHD1*, *SRSF9*, and *TMBIM6*, which were identified as good endogenous controls for studying hypoxia in cervical cancer, and six classifier genes (Supplementary Table S2). Minus reverse transcriptase controls were tested for residual genomic DNA for all TaqMan assays. Non-template controls without RNA into the cDNA synthesis were included. All negative controls had undetermined quantification cycle (*C<sub>q</sub>*). The data were analyzed using the comparative *C<sub>q</sub>* method (32) by normalizing the *C<sub>q</sub>* value of each classifier gene to the average *C<sub>q</sub>* value of the three reference genes:  $dC_{q, \text{gene}} = C_{q, \text{gene}} - (C_{q, \text{CHCHD1}} + C_{q, \text{SRSF9}} + C_{q, \text{TMBIM6}})/3$ . All samples were run in duplicate. Samples with mean *C<sub>q</sub>* > 37 or SD > 0.4 were excluded.

### Gene expression classifier

To construct a gene classifier for separating the more and less hypoxic tumors, a previously presented algorithm (11) was utilized with small modifications, as described in Supplementary Document S1. *A<sub>Brix</sub>* was used as a measure of hypoxia, and the construction was performed blinded to the clinical outcome. In brief, the classifier consisted of three parameters for each gene included, that is, the mean expression of the gene in a group of more hypoxic tumors ( $\mu_{\text{more}}$ ) and a group of less hypoxic tumors ( $\mu_{\text{less}}$ ) and its common variance (*W*) across both groups. The classifier parameters were determined as described below based on the training cohort, which was assumed to represent a typical patient cohort, and tabulated for further use in the classification of new tumors.

For a new tumor to be classified, the expression of each classifier gene in this tumor was compared with the tabulated classifier parameters  $\mu_{\text{more}}$  and  $\mu_{\text{less}}$  of the same gene, using the third classifier parameter, *W*, as weighting factor. This was performed for all classifier genes, and two expression distances, *D<sub>more</sub>* and *D<sub>less</sub>*, were calculated for the tumor:

$$D_i = \sum_m \frac{(y_m - \mu_{im})^2}{W_m}$$

where *i* is the more or less hypoxic group, *m* is the *m*th gene in the classifier,  $\mu_{im}$  is the tabulated mean expression of gene *m* in group *i*, *y<sub>m</sub>* is the expression of gene *m* in the tumor being classified, and *W<sub>m</sub>* is the tabulated common variance of gene *m*. The tumor was classified into the group for which the *D* value was smallest, and hence, the weighted gene expressions were closest. Thus, by considering the difference *D<sub>less</sub>* - *D<sub>more</sub>*, tumors with a negative difference were classified as less hypoxic, whereas tumors with a positive difference were classified as more hypoxic. The classification threshold is therefore zero for the *D<sub>less</sub>* - *D<sub>more</sub>* difference and predefined by the method.

To determine the classifier parameters, we defined the more and less hypoxic groups in the training cohort by separating the tumors into a low and high *A<sub>Brix</sub>* group, respectively. A leave-one-out cross-validation approach was used to determine both the optimal separation of the two groups based on *A<sub>Brix</sub>* and which genes to include in the classifier to achieve correct classification according to *A<sub>Brix</sub>* in the same analysis (Supplementary Document S1). The classifier parameters  $\mu_{\text{more}}$ ,  $\mu_{\text{less}}$ , and *W* were then determined for each classifier gene in the training cohort and tabulated (Table 1).

The classifier parameters are specific for the Illumina WG-6 assay. To use the classifier on Illumina HT-12 and RT-qPCR data, transformation of the gene expression levels was performed before calculation of the *D* values (Supplementary Document S2).

### Statistical analysis

Clinical endpoints were progression-free survival (PFS), locoregional control (LRC), and disease-specific survival (DSS) for follow-up until 5 years. For patients with less than 5 years of follow-up, status was assessed on October 3, 2014. Patients were censored at their last appointment or at 5 years. For PFS, time from diagnosis to disease-related death or first event of relapse was used, LRC was defined as control within the irradiated pelvis, and DSS was defined as not dead from cervical cancer. Deaths within 2 years after inclusion were regarded as disease related unless another cause was documented.

Associations were estimated by Spearman rank correlation or Pearson correlation, and differences between groups were assessed with Fisher exact test. A competing risk model was used for calculating cumulative incidence, with death from other causes than cervical cancer as competing event. Fourteen of the 281 patients died of other causes within the follow-up period of 5 years. Gray test was used to assess differences between cumulative incidence curves. Cox uni- and multivariate proportional hazard (PH) analyses were performed, and assumptions of PHs were tested graphically using log-minus-log plots. Existing clinical markers, that is, tumor volume, Federation International de Gynecologie et d'Obstetrique (FIGO) stage, and lymph node involvement, were used as covariates to evaluate the independent prognostic value of the classifier. Significance level was 5%, and all *P* values were two sided. Cox PH analyses were performed in SPSS Statistics 21, whereas all other analyses were performed using R (33) version 3.1.1.

## Results

### Classifier construction

The classifier was based on a 31-gene signature identified in previous work (Fig. 1; ref. 20). To enrich for genes specific for hypoxia in cervical cancer, the 31-gene signature was first reduced to include only the 17 genes with at least a 2-fold upregulation by hypoxia in at least one of eight cervical cancer cell lines (Supplementary Table S3). These 17 genes served as a basis for classifier construction in the training cohort. We found an optimal separation of the cohort into 11 more hypoxic (low  $A_{\text{Brix}}$ ) and 31 less hypoxic (high  $A_{\text{Brix}}$ ) tumors (Fig. 2A; Supplementary Document S1). This separation led to correct classification in 33 to 34 of the 42 leave-one-out classifications when including the 5 to 12 top-ranked genes in the classifier (Fig. 2A). To determine how many genes to include in the classifier, the ranking of the genes was recorded for the 42 leave-one-out classifications (Supplementary Document S1). For the 6-gene classifier, the same genes were present in at least 41 of the classifications. Results for the other candidates were slightly less stable, and the final classifier was chosen to consist of these six genes (*ERO1A*, *DDIT3*, *KCTD11*, *P4HA2*, *STC2*, *UPK1A*; Fig. 2B; Supplementary Document S1).

On the basis of the expression levels of the six genes in a new tumor and the classifier parameters,  $\mu_{\text{more}}$ ,  $\mu_{\text{less}}$ , and  $W$  for each gene (Table 1), the expression distances  $D_{\text{more}}$  and  $D_{\text{less}}$  can be calculated for the independent tumor and its similarity to the more and less hypoxic groups determined.  $D_{\text{less}}-D_{\text{more}}$  represents degree of this similarity and is linearly correlated with the gene expression levels ( $P < 0.001$ ;  $r = 0.99$ ;  $n = 42$ ; Supplementary Document S1). Classification of the tumors in the training cohort resulted in  $D_{\text{less}}-D_{\text{more}}$  values from  $-22.0$  to  $18.6$  (Fig. 2C, left). Tumors with different  $D_{\text{less}}-D_{\text{more}}$  values showed differences in the  $A_{\text{Brix}}$  map (examples in Fig. 2C, right), and  $D_{\text{less}}-D_{\text{more}}$  showed a significant association to  $A_{\text{Brix}}$  ( $P < 0.001$ ;  $\rho = -0.66$ ;  $n = 42$ ; Fig. 2C, left) that was just as strong as for the original 31-gene signature (20) represented by a gene score ( $P < 0.001$ ;  $\rho = -0.68$ ;  $n = 42$ ). The association to  $A_{\text{Brix}}$  was thus retained after reducing the signature and constructing the classifier.

### Validation across cohorts and array generations

The prognostic significance of the classifier was evaluated in two independent datasets based on different Illumina array generations (WG-6 and HT-12; Fig. 1). For cohort 1, assayed using the

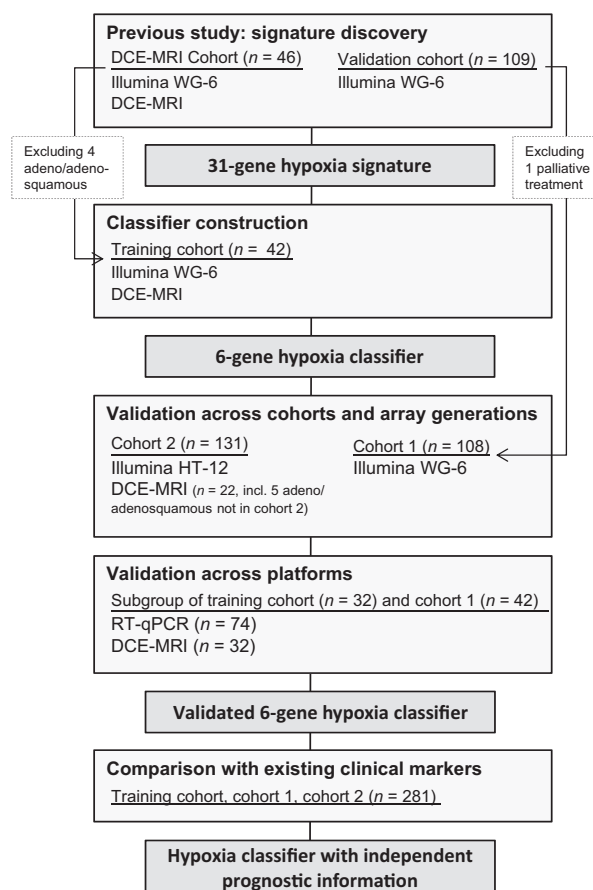


**Figure 1.**

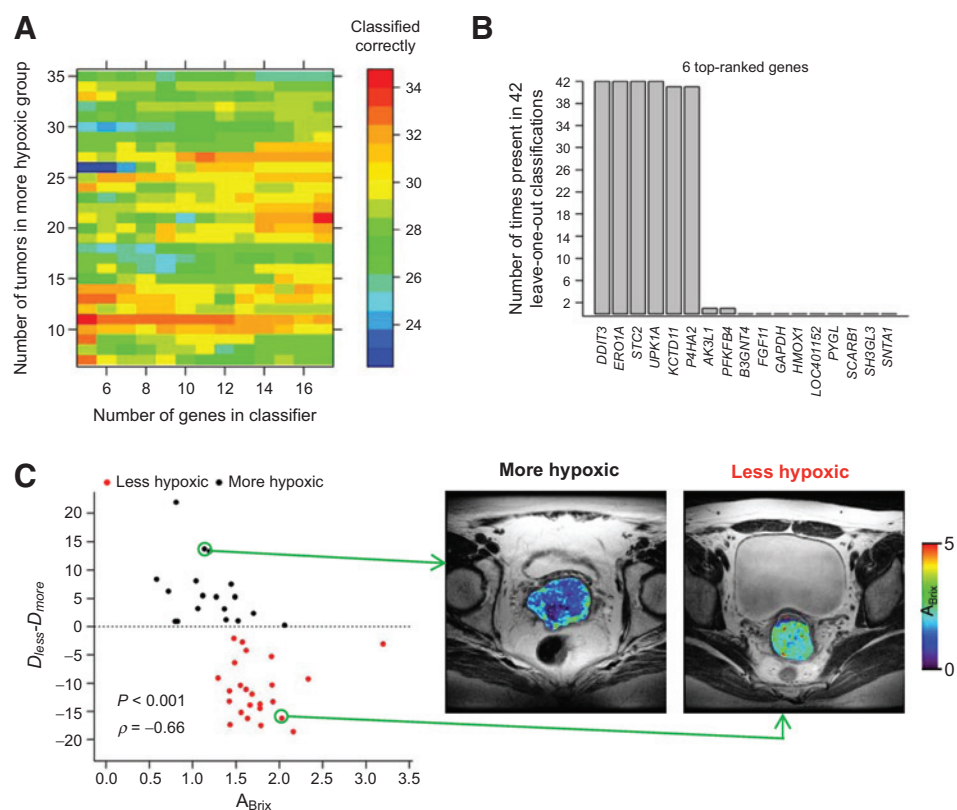
Schematic overview of study cohorts and stages. A previously determined and validated prognostic 31-gene hypoxia signature associated with the DCE-MRI parameter  $A_{\text{Brix}}$  (20) was used as basis for constructing a hypoxia classifier. The 31 genes were first reduced to 17 by excluding genes not regulated by hypoxia in cervical cancer cell lines (not shown). The classifier was constructed and its  $A_{\text{Brix}}$  association confirmed in a training cohort. The 6-gene classifier was validated across cohorts and Illumina array generations (WG-6 and HT-12), the prognostic value in cohort 1 and cohort 2, and the  $A_{\text{Brix}}$ -association for a subset of the patients in cohort 2 and five adeno/adenosquamous carcinomas. The robustness of the classifier across platforms was addressed using RT-qPCR on a subset of the patients assayed with the WG-6 assay. The prognostic value of the classifier for different endpoints and in comparison with existing clinical markers was assessed in the combined cohort of all patients.

WG-6 arrays, 40 of 108 patients (37%) were classified with a more hypoxic tumor. In this group, a significantly higher cumulative incidence of recurrence was found than in the less hypoxic group [40% vs. 15% at 5 years;  $P = 0.0035$ ; HR, 3.06; 95% confidence interval (CI), 1.39–6.74; Fig. 3A]. Thus, the classifier could separate the patients into two groups with different outcome similarly to the original 31-gene hypoxia score (Fig. 3B), showing that the prognostic value of the signature was retained in the 6-gene classifier.

Of the 131 tumors in cohort 2, assayed by HT-12 arrays, 42 (32%) were classified as more hypoxic, and the patients in the more hypoxic group had a significantly higher risk of relapse than the others (36% vs. 20% at 5 years;  $P = 0.014$ ; HR, 2.42; 95% CI, 1.20–4.90; Fig. 3C). In comparison, separation of patients based

**Figure 2.**

Classifier construction in the training cohort. **A**, number of tumors classified correctly according to  $A_{\text{Brix}}$  in 42 leave-one-out classifications using classifiers with 7–35 tumors in the more hypoxic group and the 5–17 top-ranked genes. The data revealed the optimal separation of the 42 tumors in the training cohort into 11 more (low  $A_{\text{Brix}}$ ) and 31 less (high  $A_{\text{Brix}}$ ) hypoxic tumors (red/orange color for 5–12 genes). **B**, number of times each gene was ranked among the top six genes in the 42 leave-one-out classifications for the optimal separation. Gene symbols are indicated. **C**, classification of the 42 tumors used for classifier construction. Correlation between  $A_{\text{Brix}}$  and  $D_{\text{less}}-D_{\text{more}}$  (left). Spearman rank correlation coefficient ( $\rho$ ) and  $P$  value are listed. Stippled line, predefined classification threshold of zero for  $D_{\text{less}}-D_{\text{more}}$ .  $A_{\text{Brix}}$ -map superimposed on T2-weighted MR image for two tumors classified as more hypoxic and less hypoxic, respectively (right).



NOTE: The classifier parameters  $\mu_{\text{more}}$ ,  $\mu_{\text{less}}$ , and W were derived from the training cohort with 11 more hypoxic (low  $A_{\text{Brix}}$ ) and 31 less hypoxic (high  $A_{\text{Brix}}$ ) tumors based on Illumina WG-6 expression array data.

<sup>a</sup>HUGO gene symbols are provided. Previous gene symbol for *ERO1A* was *ERO1L*.

on the original 31-gene hypoxia score with the same threshold as in Fig. 3B gave a smaller, not statistically significant difference between the groups (31% vs. 18% at 5 years;  $P = 0.13$ ; HR = 1.75; CI, 0.84–3.66). Moreover, a significant correlation between  $A_{\text{Brix}}$  and  $D_{\text{less}}-D_{\text{more}}$  was found in a subgroup of the patients with available  $A_{\text{Brix}}$  data ( $P = 0.027$ ;  $\rho = -0.47$ ;  $n = 22$ ; Fig. 3D). These findings validated the prognostic significance and the  $A_{\text{Brix}}$  association of the classifier and demonstrated its robustness across array generations.

We evaluated the ability of the classifier to predict the hypoxia status defined by  $A_{\text{Brix}}$  using all 64 tumors with available  $A_{\text{Brix}}$  data. Forty-nine out of 64 tumors were correctly classified according to  $A_{\text{Brix}}$ , giving an accuracy of 0.77. Hence, there was a statistically significant association between classifier- and  $A_{\text{Brix}}$ -based classification ( $P < 0.001$ ; Supplementary Table S4). Furthermore, the classifier identified most of the  $A_{\text{Brix}}$ -defined more hypoxic tumors correctly with a sensitivity of 0.93 but also classified some of the  $A_{\text{Brix}}$ -defined less hypoxic tumors as more

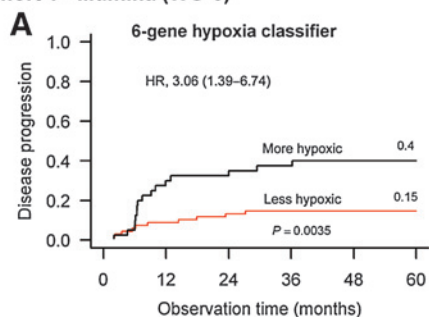
hypoxic, resulting in a precision of 0.48 and a specificity of 0.72 for this group (Supplementary Table S5). The precision of less hypoxic classification was 0.97, showing that almost all of the tumors classified as less hypoxic were correctly classified according to  $A_{\text{Brix}}$ . Of importance, the  $D_{\text{less}}-D_{\text{more}}$  value and/or the  $A_{\text{Brix}}$  value of most of the incorrectly classified tumors were close to the borders between the more and less hypoxic groups, and as many as 6 of the 14 tumors incorrectly classified as more hypoxic experienced relapse (Supplementary Fig. S1).

#### Validation across platforms

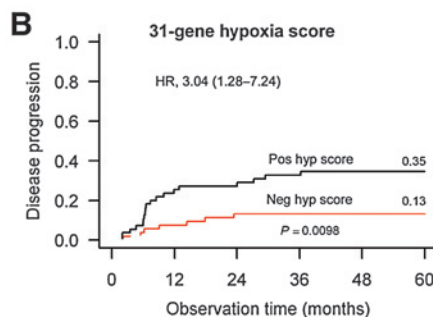
To further evaluate its robustness, a technical transfer of the classifier to RT-qPCR was performed for 74 patients (Fig. 1). For 19 of the 74 samples, gene expression measurements for *KCTD11* and/or *UPK1A* were unsuccessful. The robustness of the classifier when lacking *UPK1A* and/or *KCTD11* as compared with the full 6-gene classifier was estimated from the Illumina data of the 281 patients included in the study. Prognostic significance was

Fjeldbo et al.

## Cohort 1 - Illumina (WG-6)

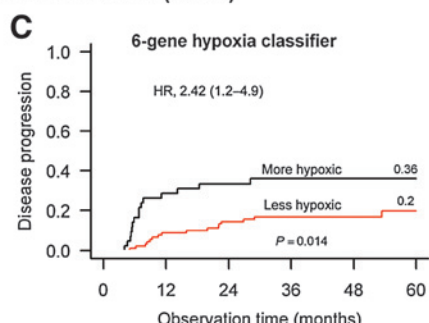


No. at risk	0	12	24	36	48	60
Less hypoxic	68	61	57	53	46	36
More hypoxic	40	28	27	24	22	18



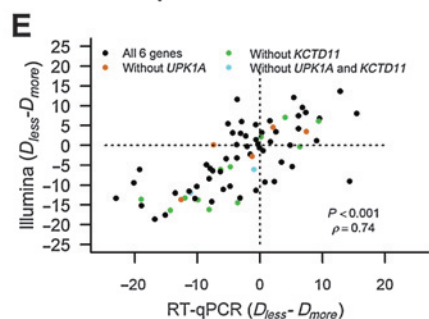
No. at risk	0	12	24	36	48	60
Neg hyp score	53	49	46	43	38	31
Pos hyp score	55	40	38	34	30	23

## Cohort 2 - Illumina (HT-12)

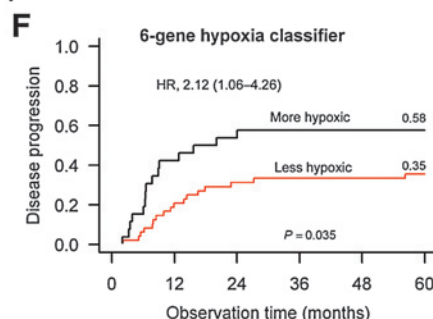


No. at risk	0	12	24	36	48	60
Less hypoxic	89	81	75	61	33	27
More hypoxic	42	30	27	22	16	9

## Illumina vs. RT-qPCR



## RT-qPCR



No. at risk	0	12	24	36	48	60
Less hypoxic	48	38	33	30	29	24
More hypoxic	26	15	12	9	9	9

## Figure 3.

Classifier performance in two independent cohorts and across platforms. Cumulative incidence of disease progression for cohort 1 patients ( $n = 108$ ) classified by the 6-gene classifier (A) and the original 31-gene hypoxia (hyp) signature (B), and cohort 2 patients ( $n = 131$ ) classified by the 6-gene classifier (C). Gene expression was measured using Illumina WG-6 (cohort 1) or HT-12 (cohort 2) arrays. D, correlation between  $A_{Brix}$  and  $D_{less-D_{more}}$  for a subgroup of 17 cohort 2 patients and 5 patients with adeno/adenosquamous carcinoma. Spearman rank correlation coefficient ( $\rho$ ) and  $P$  value are listed. Stippled line, predefined classification threshold of zero for  $D_{less-D_{more}}$ . E, correlation between  $D_{less-D_{more}}$  based on Illumina WG-6 and RT-qPCR ( $-dC_q$ ) data for 74 patients. In the Illumina assay, data for all 6 genes were available. In the RT-qPCR assay, 55 patients were classified by all 6 genes (black dots), 12 patients without *KCTD11* only (green dots), 5 without *UPK1A* only (brown dots), and 2 without both *KCTD11* and *UPK1A* (blue dots). Correlation coefficient ( $\rho$ ) and  $P$  value for Spearman rank correlation are listed. Stippled lines, predefined classification threshold of zero for  $D_{less-D_{more}}$ . F, cumulative incidence of disease progression for 74 patients classified by the 6-gene classifier with RT-qPCR data. A, B, C, and F, 60-month recurrence probability, 95% CIs for HR,  $P$  values from Gray test, and number of patients at risk are indicated; death from other causes than cervical cancer was included as a competing event ( $n = 9$  in cohort 1 and 3 in cohort 2).

obtained for all four combinations of the 4–6 genes (Supplementary Table S6). All 74 patients could therefore be classified on the basis of the data of 4–6 genes. The expression levels of the six classifier genes showed a strong correlation between the RT-qPCR and Illumina WG-6–based measurements, with a Spearman rank correlation coefficient above 0.7 (Supplementary Fig. S2). Moreover, there was a significant correlation between the Illumina-based and RT-qPCR–based classifications ( $P < 0.001$ ;  $\rho = 0.74$ ; Fig. 3E). Of 74 patients, 56 (75.7%) were classified to the same group by the RT-qPCR and Illumina assay (Supplementary Table S7), showing reproducibility of the classifier using two different assays ( $P < 0.001$ ). For the remaining 18 patients, 11 were classified with a more hypoxic tumor by Illumina and not by RT-qPCR, whereas 7 were classified with a more hypoxic tumor by

RT-qPCR and not by Illumina. For many of the patients classified differently with the two methods,  $D_{less-D_{more}}$  was close to the border between the two groups (Fig. 3E). Moreover, the few patients with missing RT-qPCR data for one or two genes were not classified differently as compared with the others (Fig. 3E), illustrating the robustness of the classifier in that missing values can be tolerated.

The 26 patients (35%) classified to the more hypoxic group by RT-qPCR had a poor prognosis compared with the others (58% vs. 35% at 5 years;  $P = 0.035$ ; HR = 2.12; CI, 1.06–4.26; Fig. 3F), and the separation between the groups were similar to that obtained with Illumina data for the same patients (58% vs. 34% at 5 years; Supplementary Fig. S3A). Also the  $A_{Brix}$  association could be validated across the platforms, although

**Table 2.** Patient and tumor characteristics for 281 patients classified with a more or less hypoxic tumor by the 6-gene classifier based on Illumina BeadArray data

Characteristic	All patients (n = 281)	More hypoxic (n = 100)	Less hypoxic (n = 181)	P <sup>a</sup>
	n (%)	n (%)	n (%)	
Age (years)				1.00
Median	54.5	54.4	54.7	
Range	21.8–84.2	21.8–83.9	24.3–84.2	
<54.5 years	140 (50)	50 (50)	90 (50)	
≥54.5 years	141 (50)	50 (50)	91 (50)	
FIGO stage				0.037
IB–IIB	202 (72)	64 (64)	138 (76)	
IIIA–IVA	79 (28)	36 (36)	43 (24)	
Tumor volume (cm <sup>3</sup> ) <sup>b</sup>				0.0019
Median	36.8	53.8	28.3	
Range	1.9–321.0	5.3–321.0	1.9–302.0	
<36.8 cm <sup>3</sup>	132 (50)	34 (37)	98 (57)	
≥36.8 cm <sup>3</sup>	132 (50)	59 (63)	73 (43)	
Pelvic lymph node status <sup>c</sup>				0.032
Positive	121 (43)	52 (52)	69 (38)	
Negative	160 (57)	48 (48)	112 (62)	

<sup>a</sup>Fisher exact test for comparisons between the more and less hypoxic group.

<sup>b</sup>Determined from pretreatment MR images. Calculated based on 3 orthogonal diameters (a, b, c) as  $(\pi/6)abc$ . Tumor volume was undetermined for 17 tumors due to lack of MRI: 7 in the more and 10 in the less hypoxic group.

<sup>c</sup>Determined from pretreatment MR or, for 17 patients, CT images.

the correlation was somewhat stronger for Illumina WG-6 ( $P < 0.001$ ;  $\rho = -0.70$ ;  $n = 32$ ) than RT-qPCR ( $P = 0.003$ ,  $\rho = -0.51$ ;  $n = 32$ ; Supplementary Fig. S3B and S3C).

### Comparison with clinical markers

To compare classifier performance with existing clinical markers, all cohorts were merged (Fig. 1). Of 281 patients, 100 (36%) were classified with a more hypoxic tumor. The probabilities of having high tumor stage, large tumor volume, or lymph node involvement were significantly higher for the more hypoxic group compared with the less hypoxic group (Table 2). Among the patients in the more hypoxic group, 36% had a stage IIIA–IVA tumor, 63% had a tumor volume above the median value of 36.8 cm<sup>3</sup>, and 52% had lymph node involvement at the time of diagnosis as compared with 24%

( $P = 0.037$ ), 43% ( $P = 0.0019$ ), and 38% ( $P = 0.032$ ) in the less hypoxic group.

In univariate Cox regression analyses, both the clinical markers and 6-gene classifier showed prognostic significance regardless of endpoint, with HRs above 2 (Table 3). Moreover, the significance of the classifier was retained in multivariate analyses, with HRs of 2.12 (PFS), 2.62 (LRC), and 2.12 (DSS; Table 3). Thus, even though there were associations between hypoxia classification and the other markers, the classifier emerged as an independent prognostic factor at all endpoints.

### Discussion

Our study is the first to construct a classifier for assessing hypoxia-related risk of chemoradiotherapy failure in cervical

**Table 3.** Cox regression analyses based on 281 patients

Factor	Univariate analysis		Multivariate analysis <sup>a</sup>	
	P	HR (95% CI)	P	HR (95% CI)
PFS				
Lymph node status	<0.001	2.29 (1.45–3.61)	N.S.	—
Tumor volume <sup>b</sup>	<0.001	3.47 (2.05–5.87)	0.004	2.26 (1.30–3.95)
FIGO stage <sup>c</sup>	<0.001	4.12 (2.63–6.47)	<0.001	3.19 (1.95–5.21)
6-gene hypoxia classifier <sup>d</sup>	<0.001	2.46 (1.57–3.85)	0.002	2.12 (1.33–3.40)
LRC <sup>e</sup>				
Lymph node status	0.004	3.07 (1.44–6.57)	(0.056)	2.16 (0.98–4.73)
Tumor volume <sup>b</sup>	0.015	2.67 (1.21–5.91)	N.S.	—
FIGO stage <sup>c</sup>	0.001	3.21 (1.56–6.59)	0.007	2.85 (1.34–6.07)
6-gene hypoxia classifier <sup>d</sup>	0.002	3.23 (1.56–6.72)	0.012	2.62 (1.23–5.58)
DSS				
Lymph node status	<0.001	2.60 (1.55–4.36)	(0.095)	1.62 (0.92–2.84)
Tumor volume <sup>b</sup>	<0.001	4.11 (2.21–7.65)	0.021	2.21 (1.13–4.34)
FIGO stage <sup>c</sup>	<0.001	5.01 (3.02–8.31)	<0.001	3.58 (2.03–6.23)
6-gene hypoxia classifier <sup>d</sup>	<0.001	2.70 (1.63–4.46)	0.006	2.12 (1.24–3.61)

Abbreviation: N.S., non-significant.

<sup>a</sup>In the multivariate analyses, the same results were obtained for forward and backward selection.

<sup>b</sup>Patients were divided into two groups based on the median tumor volume of 36.8 cm<sup>3</sup>. Tumor volume was undetermined for 17 patients.

<sup>c</sup>Patients were divided into two groups based on a FIGO stage of IB–IIB and IIIA–IVA.

<sup>d</sup>Patients were classified into two groups, one group with less hypoxic tumors and one with more hypoxic tumors.

<sup>e</sup>Location of recurrence was unknown for 3 patients.

cancer. By focusing on an aggressive phenotype, rather than solely on the patient outcome, which is often done in development of prognostic tests (25, 34), our classifier may be more robust against possible gradual improvements in diagnostics and treatment over time. Furthermore, to our knowledge, our approach is the first to combine functional imaging and gene expression variations in the construction of a gene classifier for clinical use. Correlation analyses of image features and gene expression have proven powerful in exploration of the molecular background of the images by us (20) and others (35). Here, we demonstrate a novel way of combining imaging and gene expression to construct a genomic tool for utilization in the treatment decision making both alone and with a potential for future integration with DCE-MRI.

The gene classifier was constructed by using the DCE-MRI parameter  $A_{\text{Brix}}$  as an independent measure of tumor hypoxia. Previously identified  $A_{\text{Brix}}$ -associated hypoxia-responsive genes (20) were used as potential classifier genes, and the final classifier consisted of six genes that together showed the best separation of the tumors in the training cohort according to hypoxia status. A new tumor was evaluated by comparing the expression levels of these genes with the tabulated mean levels (classifier parameters), determined for the more and less hypoxic groups in the training cohort, using a predefined threshold of zero for the output,  $D_{\text{less}} - D_{\text{more}}$ , to classify the tumor as more or less hypoxic. Hence, our dichotomous classifier with a predefined threshold would be easy to interpret and applicable in a prospective setting in the clinic.

Application of the classifier in different cohorts and test assays suggested that the method provides a robust assessment of hypoxia-related aggressiveness. Associations with outcome were demonstrated for two cohorts recruited over a time period of 11 years, during which MR image-guided brachytherapy has been implemented in our hospital and replaced brachytherapy based on 2D X-ray imaging (36). Moreover, the second cohort was analyzed with another Illumina array generation, which required data transformation prior to classification. Successful utilization of the classifier was also demonstrated in a RT-qPCR assay, with samples collected over a period of 8 years. In all tests of the classifier, not only its prognostic impact but also its association to  $A_{\text{Brix}}$  was retained. Notably, the classifier seemed to be more robust than the original 31-gene score, for which association to clinical outcome failed to reach statistical significance in the second cohort.

The classifier was associated with outcome independent of conventional markers for PFS, LRC, and DSS and may provide information about disease progression that is not covered by current diagnostics. Even though FIGO is a strong prognostic factor in cervical cancer, the classifier emerged as an independent prognostic factor. Importantly, through its biologic fundament, the classifier could be a well-needed tool for selecting patients to hypoxia-modifying adjuvant therapy and to avoid added side effects to those who are not expected to respond. The latter scenario is important because the risk of damage to critical pelvic organs is already a significant challenge in the conventional chemoradiotherapy (1, 2, 37). In addition, many patients classified with hypoxia in our work had a high risk of both failure and side effects by conventional markers, presented with large tumor, lymph node involvement, and/or stage III or IV disease. These patients belong to a group where the gain of treatment improvements would be particularly high (1, 2). A higher incidence of

lymph node-positive patients in the more hypoxic group and a weak correlation between hypoxia and tumor size have been found in earlier cervical cancer studies using oxygen electrodes to assess hypoxia (4, 38, 39), in accordance with our findings.

Hypoxia gene signatures have been constructed in other tissue types by different approaches, and some signature genes are in common. Among 32 signatures reviewed by Harris and colleagues (19), two of our six classifier genes, *P4HA2* and *ERO1A*, are among the 20 most frequently appearing ones. The presence of common genes indicates that it might be possible to identify a signature that is applicable in different tumor sites, which has indeed been demonstrated in some cases (10, 15, 17, 40, 41). However, although the head and neck cancer signature by Eustace and colleagues identified patients with laryngeal cancer who seemed to benefit from adjuvant hypoxia-modifying treatment, this was not the case when the signature was used on patients with bladder cancer (12). Moreover, when comparing six of the previously published hypoxia gene signatures (10–15) with the classifier genes in this work, we found that our genes had the strongest prognostic impact in the cervical cancer dataset (Supplementary Document S3). In particular, only the signature developed in breast cancer by Hu and colleagues (15) showed a significant association to outcome ( $P = 0.026$ ) in Cox PH univariate analysis. Out of our classifier genes, only *KCTD11* and *P4HA2* were present in three (10–12) or one (11) of the six signatures, respectively. These results support the view that there are molecular differences in the aggressive hypoxic phenotype across cancers (19) and that cancer-type specific hypoxia gene classifiers are more effective (18). Furthermore, although some of the other signatures were statistically significantly correlated with  $A_{\text{Brix}}$  (Supplementary Document S3), the signature of our classifier genes showed a stronger  $A_{\text{Brix}}$ -association and was thus the best one for describing the aggressive phenotype reflected in the DCE-MR images of cervical cancer.

The gene classifier appeared to classify a higher number of tumors as more hypoxic compared with  $A_{\text{Brix}}$ -based classification, and there might be an intermediate group that should be handled separately in a clinical trial. However, as 43% of the tumors classified as more hypoxic only with the classifier experienced recurrence, we speculate that the classifier might be a better method for identifying the aggressive hypoxic tumors than  $A_{\text{Brix}}$ . Furthermore, the classifier was shown to have a high precision in classifying the less hypoxic tumors, thus correctly identifying the patients that may not benefit from hypoxia-modifying treatment and potentially sparing many patients for unnecessary toxicity. A combination of the gene classifier with DCE-MRI-based hypoxia evaluation for improved prediction of hypoxia-related failure would be of interest to evaluate in future work.

The Brix model used to calculate  $A_{\text{Brix}}$  represents a simplistic description of the uptake of contrast agent in tumors (21), and this weakness in the DCE-MRI analysis might explain why  $A_{\text{Brix}}$  failed to identify some of the aggressive tumors detected only with the classifier. This limitation of our work needs to be addressed before a multifactorial tool based on the combined use of our classifier and imaging can be developed for clinical use. Furthermore, the predictive value of the classifier in identifying the tumors that will benefit from hypoxia-modifying treatment remains to be shown. Two head and neck cancer signatures have shown promise as predictive hypoxia

biomarkers (12, 42, 43), illustrating the potential of gene signatures for hypoxia stratification. For cervical cancer, the optimal hypoxia-targeting drug has yet to be defined (7, 8), and careful considerations in the study design have to be done due to toxicity problems. Future work should involve multicenter studies for verifying the classifier's prognostic value and testing the predictive impact in a clinical trial.

The classifier genes provide biologic insight into the disease that may aid the choice of drugs for combination trials. *STC2*, *P4HA2*, and *ERO1A* have been identified as direct target genes of the hypoxia-inducible factor 1 (HIF1; refs. 44–47). In addition, *DDIT3* (48), *ERO1A* (49), and *STC2* (50) may be activated through the unfolded protein response (UPR). Thus, both HIF1 and UPR pathways, which are major oxygen-sensitive pathways promoting hypoxia tolerance (51), might be involved in mediating the aggressive phenotype reflected by our classifier. Several HIF1 and UPR-targeting drugs are currently under development (48, 52–54) and could be relevant to evaluate in the selected patients.

In conclusion, we have developed a prognostic gene classifier that is associated with tumor hypoxia as evaluated by DCE-MRI and can characterize a tumor as either more or less hypoxic based on the expression level of six genes in a biopsy. The classifier may give an early indication of a patient's risk of hypoxia-related recurrence and has potential to serve as a biomarker for patients that would be eligible for clinical trials testing hypoxia-modifying drugs. This could help implementing hypoxia-guided treatment strategies for patients with cervical cancer. Furthermore, the approach of combining functional imaging and gene expression variations in tumors may also be beneficial for the development of other phenotype-specific gene classifiers for clinical use.

### Disclosure of Potential Conflicts of Interest

C.H. Julin and H. Lyng are listed as inventors on a patent application covering the clinical use of the hypoxia gene signature that is owned by Oslo University Hospital (WO2013/124738).

No potential conflicts of interest were disclosed by the other authors.

### Disclaimer

The funding sources of the study have no role in the study design; in the collection, analysis, or interpretation of the data; or in the writing of the article or the decision to submit the article for publication.

### Authors' Contributions

**Conception and design:** C.S. Fjeldbo, C.H. Julin, H. Lyng

**Development of methodology:** C.S. Fjeldbo, C.H. Julin, J. Alsner

**Acquisition of data (provided animals, acquired and managed patients, provided facilities, etc.):** C.S. Fjeldbo, C.H. Julin, M.F. Forsberg, E.-K. Aarnes, G.B. Kristensen, E. Malinen

**Analysis and interpretation of data (e.g., statistical analysis, biostatistics, computational analysis):** C.S. Fjeldbo, C.H. Julin, M. Lando, M.F. Forsberg, E.-K. Aarnes, J. Alsner, E. Malinen, H. Lyng

**Writing, review, and/or revision of the manuscript:** C.S. Fjeldbo, C.H. Julin, M. Lando, M.F. Forsberg, E.-K. Aarnes, J. Alsner, G.B. Kristensen, E. Malinen, H. Lyng

**Study supervision:** H. Lyng

### Grant Support

This work was supported by The Research Council of Norway (grant no. 226120/O30), The Norwegian Cancer Society (grant no. 107438 - PR-2007-0179), and The South-Eastern Norway Regional Health Authority (grant no. 2012015).

The costs of publication of this article were defrayed in part by the payment of page charges. This article must therefore be hereby marked *advertisement* in accordance with 18 U.S.C. Section 1734 solely to indicate this fact.

Received September 25, 2015; revised March 4, 2016; accepted March 8, 2016; published OnlineFirst March 24, 2016.

### References

- Barbera L, Thomas G. Management of early and locally advanced cervical cancer. *Semin Oncol* 2009;36:155–69.
- Cannistra SA, Niloff JM. Cancer of the uterine cervix. *N Engl J Med* 1996;334:1030–8.
- Lyng H, Sundfor K, Trope C, Rofstad EK. Disease control of uterine cervical cancer: relationships to tumor oxygen tension, vascular density, cell density, and frequency of mitosis and apoptosis measured before treatment and during radiotherapy. *Clin Cancer Res* 2000;6:1104–12.
- Fyles A, Milosevic M, Hedley D, Pintilie M, Levin W, Manchul L, et al. Tumor hypoxia has independent predictor impact only in patients with node-negative cervix cancer. *J Clin Oncol* 2002;20:680–7.
- Hockel M, Schlenger K, Aral B, Mitze M, Schaffer U, Vaupel P. Association between tumor hypoxia and malignant progression in advanced cancer of the uterine cervix. *Cancer Res* 1996;56:4509–15.
- Overgaard J. Hypoxic radiosensitization: adored and ignored. *J Clin Oncol* 2007;25:4066–74.
- DiSilvestro PA, Ali S, Craighead PS, Lucci JA, Lee YC, Cohn DE, et al. Phase III randomized trial of weekly cisplatin and irradiation versus cisplatin and tirapazamine and irradiation in stages IB2, IIA, IIB, IIIB, and IVA cervical carcinoma limited to the pelvis: a Gynecologic Oncology Group study. *J Clin Oncol* 2014;32:458–64.
- Scheffer T, Winter K, Kwon JS, Stuhr K, Balaraj K, Yaremko BP, et al. RTOG 0417: efficacy of bevacizumab in combination with definitive radiation therapy and cisplatin chemotherapy in untreated patients with locally advanced cervical carcinoma. *Int J Radiat Oncol Biol Phys* 2014;88:101–5.
- Liu FF, Okunieff P, Bernhard EJ, Stone HB, Yoo S, Coleman CN, et al. Lessons learned from radiation oncology clinical trials. *Clin Cancer Res* 2013;19:6089–100.
- Winter SC, Buffa FM, Silva P, Miller C, Valentine HR, Turley H, et al. Relation of a hypoxia metagene derived from head and neck cancer to prognosis of multiple cancers. *Cancer Res* 2007;67:3441–9.
- Toustrup K, Sorensen BS, Nordmark M, Busk M, Wiuf C, Alsner J, et al. Development of a hypoxia gene expression classifier with predictive impact for hypoxic modification of radiotherapy in head and neck cancer. *Cancer Res* 2011;71:5923–31.
- Eustace A, Mani N, Span PN, Irlam JJ, Taylor J, Betts GN, et al. A 26-gene hypoxia signature predicts benefit from hypoxia-modifying therapy in laryngeal cancer but not bladder cancer. *Clin Cancer Res* 2013;19:4879–88.
- Ragnum HB, Vlatkovic L, Lie AK, Axcrone K, Julin CH, Frikstad KM, et al. The tumour hypoxia marker pimonidazole reflects a transcriptional programme associated with aggressive prostate cancer. *Br J Cancer* 2015;112:382–90.
- Ghazoui Z, Buffa FM, Dunbier AK, Anderson H, Dexter T, Detre S, et al. Close and stable relationship between proliferation and a hypoxia metagene in aromatase inhibitor-treated ER-positive breast cancer. *Clin Cancer Res* 2011;17:3005–12.
- Hu Z, Fan C, Livasy C, He X, Oh DS, Ewend MG, et al. A compact VEGF signature associated with distant metastases and poor outcomes. *BMC Med* 2009;7:9.
- Chi JT, Wang Z, Nuyten DS, Rodriguez EH, Schaner ME, Salim A, et al. Gene expression programs in response to hypoxia: cell type specificity and prognostic significance in human cancers. *PLoS Med* 2006;3:e47.

17. Buffa FM, Harris AL, West CM, Miller CJ. Large meta-analysis of multiple cancers reveals a common, compact and highly prognostic hypoxia meta-gene. *Br J Cancer* 2010;102:428–35.
18. Fardin P, Barla A, Mosci S, Rosasco L, Verri A, Versteeg R, et al. A biology-driven approach identifies the hypoxia gene signature as a predictor of the outcome of neuroblastoma patients. *Mol Cancer* 2010;9:185.
19. Harris BH, Barberis A, West CM, Buffa FM. Gene expression signatures as biomarkers of tumour hypoxia. *Clin Oncol (R Coll Radiol)* 2015; 27:547–60.
20. Halle C, Andersen E, Lando M, Aarnes EK, Hasvold G, Holden M, et al. Hypoxia-induced gene expression in chemoradioresistant cervical cancer revealed by dynamic contrast-enhanced MRI. *Cancer Res* 2012; 72:5285–95.
21. Tofts PS. Modeling tracer kinetics in dynamic Gd-DTPA MR imaging. *J Magn Reson Imaging* 1997;7:91–101.
22. Lancaster JA, Carrington BM, Sykes JR, Jones AP, Todd SM, Cooper R, et al. Prediction of radiotherapy outcome using dynamic contrast enhanced MRI of carcinoma of the cervix. *Int J Radiat Oncol Biol Phys* 2002;54:759–67.
23. Ellingson BM, Bendszus M, Boxerman J, Barboriak D, Erickson BJ, Smits M, et al. Consensus recommendations for a standardized Brain Tumor Imaging Protocol in clinical trials. *Neuro Oncol* 2015; 17:1188–98.
24. Lambin P, van Stiphout RG, Starmans MH, Rios-Velazquez E, Nalbantov G, Aerts HJ, et al. Predicting outcomes in radiation oncology—multifactorial decision support systems. *Nat Rev Clin Oncol* 2013;10:27–40.
25. Naoi Y, Noguchi S. Multi-gene classifiers for prediction of recurrence in breast cancer patients. *Breast Cancer* 2016;23:12–8.
26. Crawford ED, Scholz MC, Kar AJ, Fegan JE, Haregewoin A, Kaldate RR, et al. Cell cycle progression score and treatment decisions in prostate cancer: results from an ongoing registry. *Curr Med Res Opin* 2014;30: 1025–31.
27. Giaccia AJ. Molecular radiobiology: the state of the art. *J Clin Oncol* 2014;32:2871–8.
28. Jaffe CC. Imaging and genomics: is there a synergy? *Radiology* 2012;264: 329–31.
29. van Persijn van Meerten EL, Gelderblom H, Bloem JL. RECIST revised: implications for the radiologist. A review article on the modified RECIST guideline. *Eur Radiol* 2010;20:1456–67.
30. McShane LM, Altman DG, Sauerbrei W, Taube SE, Gion M, Clark GM. Reporting recommendations for tumor marker prognostic studies. *J Clin Oncol* 2005;23:9067–72.
31. Andersen EK, Hole KH, Lund KV, Sundfor K, Kristensen GB, Lyng H, et al. Pharmacokinetic parameters derived from dynamic contrast enhanced MRI of cervical cancers predict chemoradiotherapy outcome. *Radiother Oncol* 2013;107:117–22.
32. Livak KJ, Schmittgen TD. Analysis of relative gene expression data using real-time quantitative PCR and the 2<sup>(-Delta Delta C(T))</sup> Method. *Methods* 2001;25:402–8.
33. R Core Team: R: a language and environment for statistical computing. Vienna, Austria: R Foundation for Statistical Computing; 2015. Available from: <https://www.r-project.org/>.
34. Tramm T, Mohammed H, Myhre S, Kyndi M, Alsner J, Borresen-Dale AL, et al. Development and validation of a gene profile predicting benefit of post-mastectomy radiotherapy in high risk breast cancer patients: a study of gene expression in the DBCG82bc cohort. *Clin Cancer Res* 2014;20:5272–80.
35. Nair VS, Gevaert O, Davidzon G, Napel S, Graves EE, Hoang CD, et al. Prognostic PET 18F-FDG uptake imaging features are associated with major oncogenomic alterations in patients with resected non-small cell lung cancer. *Cancer Res* 2012;72:3725–34.
36. Tanderup K, Viswanathan AN, Kirisits C, Frank SJ. Magnetic resonance image guided brachytherapy. *Semin Radiat Oncol* 2014;24:181–91.
37. Trifiletti DM, Tyler Watkins W, Duska L, Libby BB, Showalter TN. Severe gastrointestinal complications in the era of image-guided high-dose-rate intracavitary brachytherapy for cervical cancer. *Clin Ther* 2015;37: 49–60.
38. Sundfor K, Lyng H, Trope CG, Rofstad EK. Treatment outcome in advanced squamous cell carcinoma of the uterine cervix: relationships to pretreatment tumor oxygenation and vascularization. *Radiother Oncol* 2000; 54:101–7.
39. Sundfor K, Lyng H, Rofstad EK. Tumour hypoxia and vascular density as predictors of metastasis in squamous cell carcinoma of the uterine cervix. *Br J Cancer* 1998;78:822–7.
40. Sorensen BS, Knudsen A, Wittrup CF, Nielsen S, Aggerholm-Pedersen N, Busk M, et al. The usability of a 15-gene hypoxia classifier as a universal hypoxia profile in various cancer cell types. *Radiother Oncol* 2015;116: 346–51.
41. Winther M, Alsner J, Tramm T, Nordmark M. Hypoxia-regulated gene expression and prognosis in loco-regional gastroesophageal cancer. *Acta Oncol* 2013;52:1327–35.
42. Toustrup K, Sorensen BS, Lassen P, Wiuf C, Alsner J, Overgaard J. Gene expression classifier predicts for hypoxic modification of radiotherapy with nimorazole in squamous cell carcinomas of the head and neck. *Radiother Oncol* 2012;102:122–9.
43. Hassan Metwally MA, Ali R, Kuddu M, Shouman T, Strojjan P, Iqbal K, et al. IAEA-HypoX. A randomized multicenter study of the hypoxic radiosensitizer nimorazole concomitant with accelerated radiotherapy in head and neck squamous cell carcinoma. *Radiother Oncol* 2015;116:15–20.
44. Tanimoto K, Tsuchihara K, Kanai A, Arauchi T, Esumi H, Suzuki Y, et al. Genome-wide identification and annotation of HIF-1alpha binding sites in two cell lines using massively parallel sequencing. *Hugo J* 2010;4:35–48.
45. Mimura I, Nangaku M, Kanki Y, Tsutsumi S, Inoue T, Kohro T, et al. Dynamic change of chromatin conformation in response to hypoxia enhances the expression of GLUT3 (SLC2A3) by cooperative interaction of hypoxia-inducible factor 1 and KDM3A. *Mol Cell Biol* 2012;32: 3018–32.
46. Schodel J, Oikonomopoulos S, Ragoussis J, Pugh CW, Ratcliffe PJ, Mole DR. High-resolution genome-wide mapping of HIF-binding sites by ChIP-seq. *Blood* 2011;117:e207–17.
47. Law AY, Wong CK. Stanniocalcin-2 is a HIF-1 target gene that promotes cell proliferation in hypoxia. *Exp Cell Res* 2010;316:466–76.
48. Hetz C, Chevet E, Harding HP. Targeting the unfolded protein response in disease. *Nat Rev Drug Discov* 2013;12:703–19.
49. Li G, Mongillo M, Chin KT, Harding H, Ron D, Marks AR, et al. Role of ERO1-alpha-mediated stimulation of inositol 1,4,5-triphosphate receptor activity in endoplasmic reticulum stress-induced apoptosis. *J Cell Biol* 2009;186:783–92.
50. Ito D, Walker JR, Thompson CS, Moroz I, Lin W, Veselits ML, et al. Characterization of stanniocalcin 2, a novel target of the mammalian unfolded protein response with cytoprotective properties. *Mol Cell Biol* 2004;24:9456–69.
51. Wouters BG, Koritzinsky M. Hypoxia signalling through mTOR and the unfolded protein response in cancer. *Nat Rev Cancer* 2008;8:851–64.
52. Suh DH, Kim MK, Kim HS, Chung HH, Song YS. Unfolded protein response to autophagy as a promising druggable target for anticancer therapy. *Ann N Y Acad Sci* 2012;1271:20–32.
53. Burroughs SK, Kaluz S, Wang D, Wang K, Van Meir EG, Wang B. Hypoxia inducible factor pathway inhibitors as anticancer therapeutics. *Future Med Chem* 2013;5:553–72.
54. Semenza GL. Hypoxia-inducible factors: mediators of cancer progression and targets for cancer therapy. *Trends Pharmacol Sci* 2012;33:207–14.

# Clinical Cancer Research

## Integrative Analysis of DCE-MRI and Gene Expression Profiles in Construction of a Gene Classifier for Assessment of Hypoxia-Related Risk of Chemoradiotherapy Failure in Cervical Cancer

Christina S. Fjeldbo, Cathinka H. Julin, Malin Lando, et al.

*Clin Cancer Res* 2016;22:4067-4076. Published OnlineFirst March 24, 2016.

**Updated version** Access the most recent version of this article at:  
doi:[10.1158/1078-0432.CCR-15-2322](https://doi.org/10.1158/1078-0432.CCR-15-2322)

**Supplementary Material** Access the most recent supplemental material at:  
<http://clincancerres.aacrjournals.org/content/suppl/2016/03/24/1078-0432.CCR-15-2322.DC1>

**Cited articles** This article cites 53 articles, 18 of which you can access for free at:  
<http://clincancerres.aacrjournals.org/content/22/16/4067.full#ref-list-1>

**Citing articles** This article has been cited by 4 HighWire-hosted articles. Access the articles at:  
<http://clincancerres.aacrjournals.org/content/22/16/4067.full#related-urls>

**E-mail alerts** [Sign up to receive free email-alerts](#) related to this article or journal.

**Reprints and Subscriptions** To order reprints of this article or to subscribe to the journal, contact the AACR Publications Department at [pubs@aacr.org](mailto:pubs@aacr.org).

**Permissions** To request permission to re-use all or part of this article, use this link  
<http://clincancerres.aacrjournals.org/content/22/16/4067>.  
Click on "Request Permissions" which will take you to the Copyright Clearance Center's (CCC) Rightslink site.